International Journal of Adhesion & Adhesives 136 (2025) 103889

Contents lists available at ScienceDirect

International Journal of Adhesion and Adhesives

journal homepage: www.elsevier.com/locate/ijadhadh

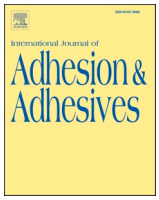

Synthesis, characterisation, and thermal degradation kinetics of lignin-based polyurethane wood adhesives

Fabio Hernández-Ramos [a,*], Bruno Esteves [b,c], Luísa Carvalho [c,d], Jalel Labidi [e], Xabier Erdocia [f]

[a] Chemical and Environmental Engineering Department. University of the Basque Country UPV/EHU. Calle Nieves Cano, 12, Vitoria-Gasteiz, Spain
[b] Centre for Natural Resources, Environment and Society-CERNAS-IPV Research Centre, Polytechnic University of Viseu, Av. Cor. José Maria Vale de Andrade, 3504-510, Viseu, Portugal
[c] Departament of Wood Engineering, Polytechnic University of Viseu, Campus Politécnico, 3504-510, Viseu, Portugal
[d] LEPABE - Faculty of Engineering and ALiCE - Associate Laboratory in Chemical Engineering, University of Porto, Rua Dr. Roberto Frias, S/n 4200-465 Porto, Portugal
[e] Chemical and Environmental Engineering Department. University of the Basque Country UPV/EHU. Plaza Europa, 1, 20018 San Sebastian, Spain
[f] Department of Applied Mathematics. University of the Basque Country UPV/EHU. Plaza Europa, 1, 20018 San Sebastian, Spain

ARTICLE INFO

Keywords:
Lignin
Bio-polyol
Polyurethane
Adhesives
Thermal degradation kinetics

ABSTRACT

Polyurethane adhesives are widely employed in a range of industrial applications due to their exceptional bonding strength, flexibility, and chemical resistance. These materials play a crucial role in wood bonding technologies, where their versatility and durability make them ideal for creating strong, long-lasting joints. In this work, Four different polyurethane wood adhesives were synthesised using ligno-based bio-polyols obtained through microwave assisted liquefaction reaction of two wood species (hardwood and softwood) using polyethylene glycol and glycerol as solvents. The reaction conditions used for the synthesis of bio-polyols were optimised in a previous work. The synthesis of polyurethanes was carried out by one-shot method using Tetrahydrofuran (THF) as solvent and MDI as diisocyanate employing different NCO:OH ratios (2.0:1, 2.5:1, and 3.0:1). The chemical structure of polyurethanes was determined through ATR-FTIR and the shear strength was analysed using Automated Bonding Evaluation System (ABES) employing beech veneer strips. Through ABES it was concluded that an NCO:OH ratio of 2.5:1 was the formulation that showed the best shear strength for a pressing time of 120 s. Employing this ratio and the same synthesis procedure, two new polyurethanes were synthesised with the bio-polyols obtained using crude glycerol instead commercial glycerol. Finally, a study of thermal degradation kinetics employing the Ozawa–Flynn–Wall (OFW) and Kissinger–Akahira–Sunose (KAS) isoconversional methods of the polyurethanes synthesised with an NCO:OH ratio of 2.5:1 was carried out. On the one hand, the E_a of each system were estimated for the different α ratios, obtaining slightly higher values for the adhesives produced using commercial glycerol than crude glycerol. In addition, the pre-exponential factor was determined, enabling an estimation of the lifetime of the polymers. This study highlights demonstrated that crude glycerol could replace commercial glycerol without compromising adhesive properties. The findings revealed that the lignin source significantly influences the adhesive's characteristics and stability, while addressing challenges in achieving industrial viability remains essential for broader application.

1. Introduction

Within the large family of plastic materials, polyurethanes (PUs), first synthesised by Dr. Otto Bayer in 1937, are of great importance to industry, as they are among the most versatile polymers due to their tuneable mechanical properties and broad range of applications such as thermoplastics, foams, elastomers, adhesives, coatings and sealants [1–3]. PUs are usually synthesised from the polyaddition reaction between polyols and a diisocyanate, with the possible addition of low molecular weight chain extender, to form repeating urethane bonds (Fig. 1) [4].

Nevertheless, such chemicals are usually obtained from petrochemical industry, which means their environmental impact is a constant concern for the chemical sector as it aims to comply with increasingly restrictive regulations. To tackle this challenge, the PU industry could consider replacing petroleum-derived polyols and isocyanates with bio-

* Corresponding author.
E-mail address: fabio.hernandez@ehu.eus (F. Hernández-Ramos).

https://doi.org/10.1016/j.ijadhadh.2024.103889
Received 27 July 2024; Received in revised form 4 November 2024; Accepted 12 November 2024
Available online 17 November 2024

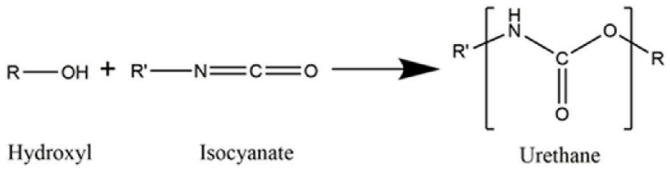

Fig. 1. Addition reaction between hydroxyl and isocyanate group to form urethane group.

based alternatives. Using more environmentally sustainable options would not only help reduce the industry's environmental footprint but could also mitigate health issues related to isocyanates, such as asthma and dermatitis [5]. Extensive research has been conducted in recent decades on the potential of obtaining these alternatives from various types of biomasses, with particular emphasis on lignocellulosic biomass, which stands out as the most promising material [6]. Among all the components of lignocellulosic biomass, lignin has generated the greatest interest for synthesising bio-based polyols that are useful for the PU industry [7]. This is mainly attributed to the following reasons: firstly, its availability, affordability, and renewable nature, as it is predominantly generated as a by-product of the Pulp & Papper industry [8]. Secondly, its phenolic structure and the abundance of both phenolic and aliphatic hydroxyl groups it contains [9]. Lignin can be used without modification, as a filler to produce PUs [10], nevertheless, these same characteristics are responsible for the low reactivity of the lignin molecule [11]. To overcome this drowback, different strategies have been developed, all aimed at increasing the molecule's reactivity. These processes can be classified into three main families: fragmentation or depolymerisation of lignin, modification to create new chemically active sites (e.g.,glyoxilation, phenolation, and hydroxymethylation) and functionalisation of hydroxyl groups [12,13]. Among the existing techniques encompassed within these three routes, liquefaction with polyhydric alcohols is one of the most widely studied strategies for synthesising polyols from lignin [14]. Furthermore, the use of lignocellulosic biomass, along with the implementation of effective strategies for the reuse or recycling of bio-polyols through processes such as glycolysis [15,16], can help minimize environmental impact, reduce waste, and optimize resource efficiency. This is because bio-polyols can be depolymerized and recovered for reuse in the production of new polyurethane products.

In this work, organosolv lignins from *Eucalyptus globulus* and *Pinus radiata* were subjected to a microwave liquefaction process using polyethylene glycol (PEG) and glycerol as organic solvents. The conditions applied were those optimised in a previous study [17]. These bio-polyols were then used to synthesise PU wood adhesives, employing MDI as diisocyanate (Fig. 2).

MDI at different NCO:OH ratios (2.0:1, 2.5:1, 3.0:1) was used in this study, identifying 2.5:1 as the optimal ratio via Automated Bonding Evaluation System (ABES). Subsequently, additional PU adhesives were developed using this ratio, substituting commercial glycerol with crude glycerol in the bio-polyol synthesis. Thus, the aim of this work was to study how this class of lignin-based bio-polyols behaves in these types of systems and how the nature of lignin can influence the microstructure, the mechanical properties and thermal properties of the polyurethanes. Characterisation included Attenuated Total Reflectance-Fourier Transform Infrared (ATR-FTIR) spectroscopy to analyse chemical structure and microphase separation; ABES to measure shear strength; and Differential Scanning Calorimetry (DSC) and Thermogravimetric Analysis (TGA) to assess thermal properties. TGA was also employed to determine degradation kinetics and estimate the lifetime of PUs using the isoconversional methods of Ozawa-Flynn-Wall (OFW) and Kissinger-Akahira-Sunose (KAS).

2. Materials and methods

2.1. Materials

Papelera Guipuzcoana Zikuñaga S.A. and Ebaki XXI S.A. provided the *Eucalyptus globulus* chips and *Pinus radiata* sawdust, respectively. The crude glycerol used in this work was obtained and characterised as described in our previous study [18]. Lignin from *Eucalyptus globulus* and *Pinus radiata* was obtained through an organosolv process following the procedure outlined in a previous study [17]. The commercial chemicals used in this work are summarised in Table 1.

Table 1
Commercial chemical compounds employed in this work.

Chemical compound	Abbreviation	Purity	Supplier
Ethanol		≥99.8 %	Scharlab
Methanol		≥99.8 %	
Dimethylformamide	DMF	HPLC ≥99.9 %	Fisher
Lithium bromide		PRS	Scientific
1,4-dioxane		≥99.8 %	
Pyridine		99.50 %	
Tetrahydrofuran	THF	Analytical reagent grade	
Phthalic anhydride		98 %	
Sulfuric acid		96 %	Panreac
Polyethylene glycol −400	PEG-400	Technical	
Glycerol	Gly	99 %	
Potassium Hydroxyde	KOH	85 %	
Sodium Hydroxyde	NaOH	>97 %	
4,4′-Methylene diphenyl diisocyanate	MDI	98 %	Merk
Dibutyltin dilaurate	DBTDL	95 %	Alfa Aesar

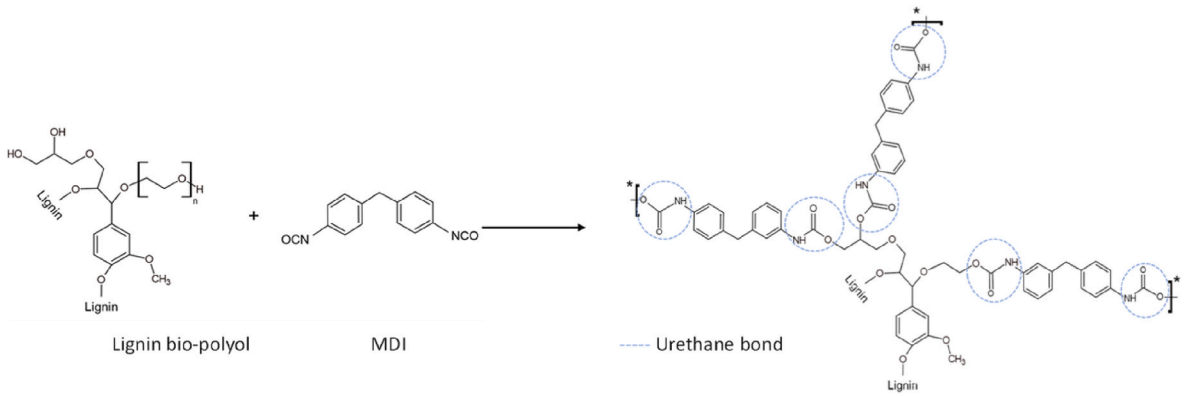

Fig. 2. Proposal for schematic formulation of a polyurethane using a lignin-based bio-polyol and MDI.

2.2. Synthesis of bio-polyols through microwave assisted liquefaction

The liquefaction of organosolv lignins from *Eucalyptus globulus* and *Pinus radiata* was performed using the reaction conditions (time: 5 min, SLR: 1/6 w/w) established in the optimisation described earlier [17], as summarised in Table 2, and following the procedure described in the same study. Nevertheless, in this instance, a CEM Microwave Discover 2.0 reactor equipped with 100 mL vessels was employed, allowing a significant ten-fold scale-up of the reaction. Triplicates of the reactions were performed.

2.3. Synthesis of lignin-based polyurethane adhesives

The synthesis of various lignin-based polyurethane adhesives (LPAs) using the aforementioned bio-polyols, namely EPE, EPE_{CG}, PPE, and $PPEC_{CG}$ was conducted employing the one-shot method under inert atmosphere (N_2) and room temperature. Initially, the bio-polyol was mixed with the THF in a three-necked round-bottomed flask and stirred vigorously, then catalyst (DBTDL) and the isocyanate (MDI) were added and stirred until the mixture reached a non-fluid state, which indicates the gel time. Three different NCO:OH ratios were employed, specifically 2.0:1, 2.5:1 and 3.0:1. For the synthesis of LPAs using EPE_{CG} and $PPEC_{CG}$, the ratio that resulted in the highest shear strength value of the PUs synthesised with EPE and PPE was selected (2.5:1). The detailed recipe for each of the synthesised LPAs is provided in Table 3.

2.4. Characterisation of the obtained bio-polyols

Important parameters, such as molecular weight distribution (M_w, M_n and PDI), hydroxyl number (I_{OH}), acid number (A_n) and functionality (*f*) of the bio-polyols obtained in the reaction scale-up, were determined following the procedure described in Ref. [17]. To obtain the average value and the standard deviation, each analysis was conducted on each triplicate of the bio-polyols.

2.5. Characterisation of lignin-based polyurethane adhesives

For ATR-FTIR, DSC, and TGA analyses, the LPAs were cured at room temperature as a film for 7 days in a Petri dish before being grounded into powder.

The LPAs were characterised using ATR-FTIR to determine both their chemical structure and their degree of microphase separation and miscibility. A PerkinElmer Spectrum Two FT-IR Spectrometer equipped with a Universal Attenuated Total Reflectance accessory provided with an internal reflection diamond crystal lens was employed. Twenty scans in transmission mode were collected with a resolution of 4 cm^{-1} over the range of 4000-600 cm^{-1}.

The shear strength of the LPAs was assessed using an automated bonding evaluation system (ABES, Adhesive Evaluation Systems, Corvallis, OR, USA) through a single lap shear test [19]. Tests were carried out employing beech (*Fagus sylvatica*) veneer strips with dimensions of 117 mm × 20 mm and a thickness of 0.5 mm. For each test, 10 mg of pre-cured adhesive was applied and spread on a wooden specimen (covering 5 mm along the edge of the beech veneer strips to cover a bonding area of 100 mm^2). A second wood strip, without adhesive, was then placed on top, ensuring both strips were properly aligned.

Table 2
Liquefaction reaction conditions optimised in a previous work [17].

Bio-polyol	EPE & EPE_{CG}	PPE & PPE_{CG}
Catalyst (% wt.)	5	3.86
Temperature (°C)	180	160
PEG/Gly or CG (% wt.)	7.57/1	7.34/1

EPE (Eucalyptus globulus Polyol for Elastic PU); PPE (Pinus radiata Polyol for Elastic PU); CG (Crude glycerol).

Table 3
Recipe used for the synthesis of LPAs.

		LPA_{EPE}	LPA_{PPE}	$LPA_{EPECG\_2.5}$	$LPA_{PPECG\_2.5}$
Bio-polyol (g)		2.5	2.5	2.5	2.5
THF (g)		1.5	1.5	1.5	1.5
DBTDL (wt%)		0.2	0.2	0.2	0.2
NCO:OH	2.0:1	3.68	2.03	–	–
	2.5:1	4.60	2.53	3.96	3.40
	3.0:1	5.52	3.04	–	–

The structure as well as the degree of micro-phase separation of the LPAs were studied by DSC using a Mettler Toledo DSC3+ instrument equipped with an electric intracooler as a refrigeration unit. Aluminium closed pans were used to encapsulate a sample weighing between 5 and 10 mg. Subsequently, two consecutive dynamic heating scans were conducted under a nitrogen atmosphere, from −80 °C to 200 °C, with a heating rate of 20 °C•min^{-1}. The glass transition temperature (T_g) of the cured LPAs was determined by identifying the inflection point on the curve during the second heating scan.

TGA of LPAs was performed employing a TGA/SDTA RSI analyser 851 (Mettler Toledo). For the analysis of the samples 3–5 mg of LPAs were heated, under N_2 atmosphere (10 mL min^{-1}), from 25 °C to 800 °C using a heating rate of 10 °C•min^{-1}. In addition, thermogravimetric analysis was employed to study the thermal degradation kinetics and the lifetime estimation of the LPAs.

To obtain the thermal degradation kinetics as well as the lifetime estimation of the PUs, the same TGA and procedure described above were employed. However, in this case, four different heating rates were used (1, 2, 5 and 10 °C•min^{-1}). For the determination of the activation energy (E_a) two different isoconversional methods were selected, namely, Ozawa-Flynn-Wall [20] (Equation (1)) and Kissinger-Akahira-Sunose [21] (Equation (2)).

In these equations, β is the heating rate, T_p is the peak exothermic temperature at a certain heating rate. E_a is the activation energy, A is the pre-exponential factor, R is the universal gas constant and $f(\alpha)$ is a function determined by the mechanism.

$$\ln(\beta) = ln\left(\frac{AE_a}{Rf(\alpha)}\right) - 5.331 - 1.052\frac{E_a}{RT_p} \quad \text{Equation 1}$$

$$\ln\left(\frac{\beta}{T_p^2}\right) = ln\left(\frac{AR}{E_a}\right) - \frac{E_a}{RT_p} \quad \text{Equation 2}$$

In both cases, the activation energy (E_a) and the preexponential factor (A) can be obtained from the slop and the intercept of the plots of $\ln(\beta)$ and $\ln\left(\frac{\beta}{T_p^2}\right)$ versus $1/T_p$.

The lifetime estimation of PUs was determined using the Ozawa's method and was calculated employing Equation (3).

$$\ln t = \frac{E}{RT} + \ln\left[-\frac{\ln(1-\alpha)}{A}\right] \quad \text{Equation 3}$$

3. Results and discussion

3.1. Bio-polyols characterisation

The bio-polyols were characterised to establish their suitability for the synthesis of polyurethane adhesives. Therefore, the molecular weight distribution (M_w, M_n, PDI), I_{OH}, A, *f*, and the chain derived from a hydroxyl group (EW) of the different samples were analysed, and a summary of the results is presented in Table 4.

As expected, the obtained results were similar to those obtained in previous works [17,18], although, due to the scale-up of the reaction, they differed slightly. Thus, the M_w was within the range required for this type of PU (2000–10000 g/mol) except for PPE_{CG}, which has a M_w of

Table 4
Characterisation of bio-polyols employed to synthesise PUs.

Sample	M_n	M_w	PDI	I_{OH}	A_n	*f*	EW
EPE	739 ± 43	3934 ± 98	5.33 ± 0.18	330 ± 3	35 ± 0.36	4.16	153.7
EPE_{CG}	852 ± 8	6644 ± 89	7.79 ± 0.18	284 ± 1	17 ± 0.24	4.29	186.4
PPE	707 ± 32	4079 ± 50	6.29 ± 0.92	182 ± 51	25 ± 0.00	2.29	271.0
PPE_{CG}	933 ± 85	11035 ± 1059	12.63 ± 0.00	182 ± 30	20 ± 0.64	2.83	277.7

M_n and M_W (g/mol), I_{OH} and A_n (mg KOH/g).

11035 g/mol [22]. As with this type of bio-polyols synthesised through liquefaction reactions, the A_n in all cases was high, but within the usual values [23]. However, the I_{OH} values were higher than 28–160 mgKOH/g, which are the values suggested for the synthesis of these PUs [24]. This is especially pronounced for EPE and EPE_{CG}, while PPE and PPE_{CG} were practically in the required range. In addition, *f* of PPE and PPE_{CG} bio-polyols was between 2 and 3 in both cases, whereas that of the EPE and EPE_{CG} bio-polyols was 4.16 and 4.29 respectively. The EW of PPE and PPE_{CG} was higher than that of EPE and EPE_{CG}, i.e., the chains derived from the hydroxyl groups of PPE and PPE_{CG} were higher than those obtained for bio-polyols synthesised with organosolv lignin from *Eucalyptus globulus* [25]. This, together with the low functionality, the I_{OH}, and M_w, suggests that PPE and PPE_{CG} bio-polyols could be more suitable for the synthesis of PU adhesives. Nevertheless, despite the higher I_{OH} and *f* values observed for the EPE and EPE_{CG} bio-polyols, which could potentially lead to a more cross-linked and rigid structure, these bio-polyols were deemed suitable for adhesive formulation.

Differences with respect to our previous studies [17,18] can be explained by the scale-up of the reaction and the type of vessel employed in each case.

3.2. Lignin-based polyurethane adhesive characterisation

A total of six LPAs were synthesised, three with each of the bio-polyols (EPE and PPE), following the procedure summarised in Table 3. Aliquots of the LPAs were taken every 30 min to monitor the reaction until the gel time was reached, after which they were analysed by ATR-FTIR. The ATR-FTIR spectra are shown in Fig. 3, and the most characteristic bands are listed in Table 5.

As observed, in all cases, as the reaction progressed in time, the band assigned to the O-H stretching (3400 cm^{-1}) decreased as a consequence of the reaction between the NCO groups of MDI and OH groups of bio-polyols to form urethane (NHCO) groups. The formation of urethane groups was confirmed by the appearance of the peaks at 3290 cm^{-1}, related to the stretching vibration of N-H groups, 1730 cm^{-1} and 1706 cm^{-1} bands corresponding to the C=O stretching vibration and the N-H bending vibration at 1507 cm^{-1} [26]. These bands increased as the isocyanate groups were consumed to form urethane bonds. It is also observable the C-N stretching bands of urethane group at 1308 cm^{-1} and 1225 cm^{-1} [10]. The C-C and C-H absorptions bands which correspond to the stretching of the aromatic ring of the MDI are observed at 1599 cm^{-1} and 1407 cm^{-1} [27].

Two noteworthy aspects should be highlighted: The first is that, surprisingly, unreacted isocyanate remained unconsumed in all of the cured LPA_{EPE} samples, while in the LPA_{PPE} samples, the band

Table 5
ATR-FTIR band assignments of PU spectra synthesised with EPE and PPE bio-polyols.

Wavenumber (cm^{-1})	Band assignment
3400	O-H stretching
3290	N-H stretching vibration of urethane groups
2970-2940-2870	CH stretching of CH_3 and CH_2
2270	Antisymetric stretching vibration of NCO
1730–1706	C=O stretching
1599	C-C stretching of the aromatic ring of MDI
1507	N-H vending vibration
1407	C-H stretching of the aromatic ring of MDI
1308	C-N stretching of urethane group
1225	C-N stretching of urethane group
1096	C-O-C stretching

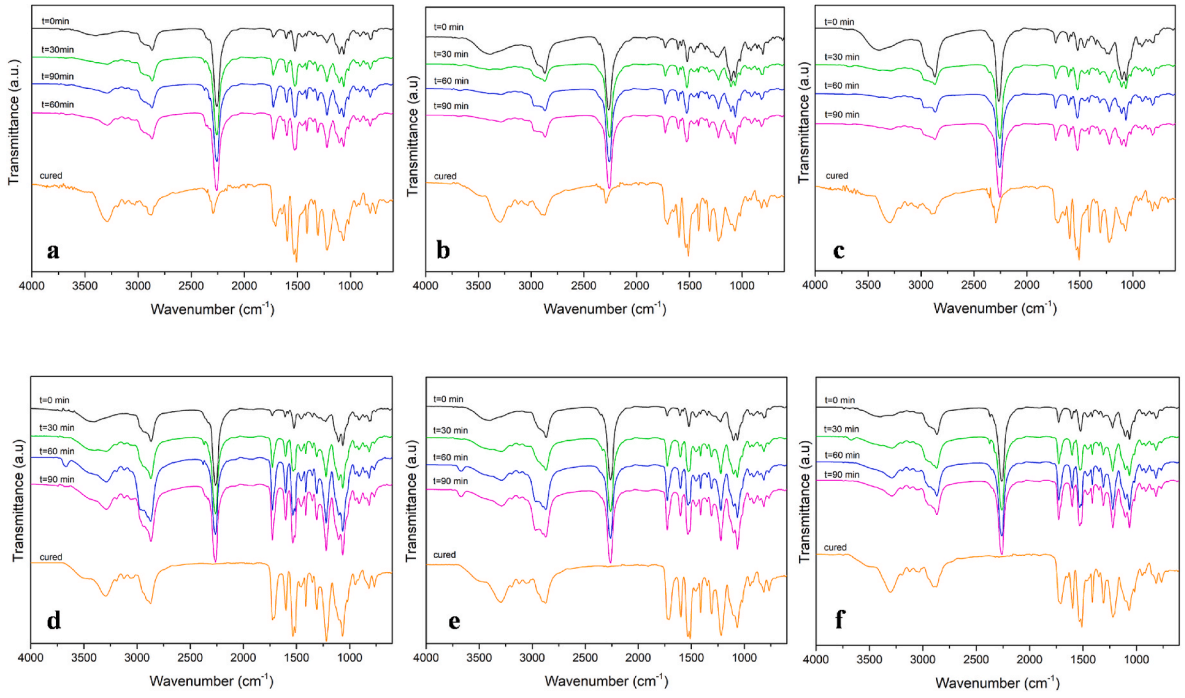

Fig. 3. ATR-FTIR spectra of the LPA formulations at different reaction times and cured. a, b, and c are the 2.0, 2.5 and 3.0 LPA_{EPE} formulations and d, e and f are the LPA_{PPE} equivalents.

corresponding to the NCO anti-symmetric vibration (2270 cm^{-1}) was not observed in the cured samples, which indicated that the polymerisation reaction was incomplete in the former. This unreacted isocyanate in the LPA_{EPE} samples is likely due to the lignin from *Eucalyptus globulus* being more sterically hindered than that from *Pinus radiata*, as the former contains more syringyl groups [28]. This unreacted isocyanate in LPA_{EPE} samples, Besides being toxic, the unreacted isocyanate in the LPA_{EPE} samples could react with the OH of the beech veneer strip or with the water adsorbed by wood, forming covalent bonds. This may increase the shear strength, leading to undesired behaviour of the PU, as it can lead to adhesives becoming stiffer and more brittle [29]. The second aspect is that, as the reaction progressed, the intensity of the bands corresponding to the C=O groups, related to free urethanes (1730 cm^{-1}) and those assigned to the urethane groups linked through hydrogen bonds (1709 cm^{-1}) [30], gradually changed.

Using ATR-FTIR spectra, the degree of separation and miscibility of the micro-phase in LPA can be determined [31]. By analysing the spectral region corresponding to carbonyl stretching, it is possible to determine the different C=O species present in LPAs. These include free C=O groups not involved in hydrogen bonding (free C=O and free C=O ester), H-bonded C=O in disordered hard segments (HS), H-bonded C=O in ordered HS, and H-bonded C=O in disordered soft segments (SS) [30]. The analysis of the micro-phase separation is interesting because the mechanical properties of PUs, among others, depend to a large extent on it [32].

Through the deconvolution of the absorbance bands of C=O groups, the degree of micro-phase separation could be determined. Curve fitting of the different cured LPAs samples was performed using a Gaussian curve model, yielding R^2 values above 0.999 in all cases. Ther resulting spectra are shown in Fig. 4. Table 6 summarises the theoretical percentage of hard segment (HS_t) for each LPA, calculated as indicated in Equation (4), along with the percentages of the different C=O species, which were calculated through the deconvolution of these bands in the ATR-FTIR spectra.

$$HS_t\ \% = \frac{nM_{MDI}}{(n+1)M_{MDI} + \overline{M}_{nPolyol}} \times 100 \qquad \text{Equation 4}$$

Where M_{MDI} is the molecular weight of the MDI diisocyanate, $\overline{M}_{nPolyol}$ is the average number molecular weight of the bio-polyol (g/mol) and n is the number of mols.

As expected, a higher NCO:OH ratio resulted in a higher HS_t content. Additionally, the percentage of HS_t was consistent for LPAs with the same isocyanate-to-hydroxyl ratio. In the LPA_{EPE} formulations, the trend for free urethane carbonyl groups in HS (C) was a general decrease. Consequently, it would be expected that the H-bonded urethane carbonyl groups (D, E and F) would be the opposite, since as the HS increases, the H-bonded urethane C=O groups tends to increase [33]. This rising trend can be observed in adhesives formulated with EPE, whereas in adhesives formulated with PPE, the 2.5:1 formulation showed the lowest value.

Following the procedure described by Ref. [34], the mass fraction of the hard and soft segments in a PU, along with their degree of micro-mixing, can be determined. This allows for the calculation of various parameters, including the proportion of H-bonded C=O groups (X_{HB}) (Equation (5)) the maximum mass fraction of the rigid segment mixed in the soft phase (W_H) (Equation (6)), assuming that all the H-bonded C=O groups are only found in the rigid domains, the weight fraction of the mixed phase (MP_W) (Equation (7)), the soft segment weight fraction (SS_W) (Equation (8)), and the hard segment weight fraction (HS_W) (Equation (9)). The corresponding values of these parameters for each formulation are indicated in Table 7.

$$X_{HB} = \frac{A_{Hb}}{K' A_{Fc} + A_{Hb}} \qquad \text{Equation 5}$$

$$W_H = \frac{(1 - X_{HB}) \times z}{[(1 - X_{HB}) \times z + (1 - z)]} \qquad \text{Equation 6}$$

$$MP_W = z \times W_H \qquad \text{Equation 7}$$

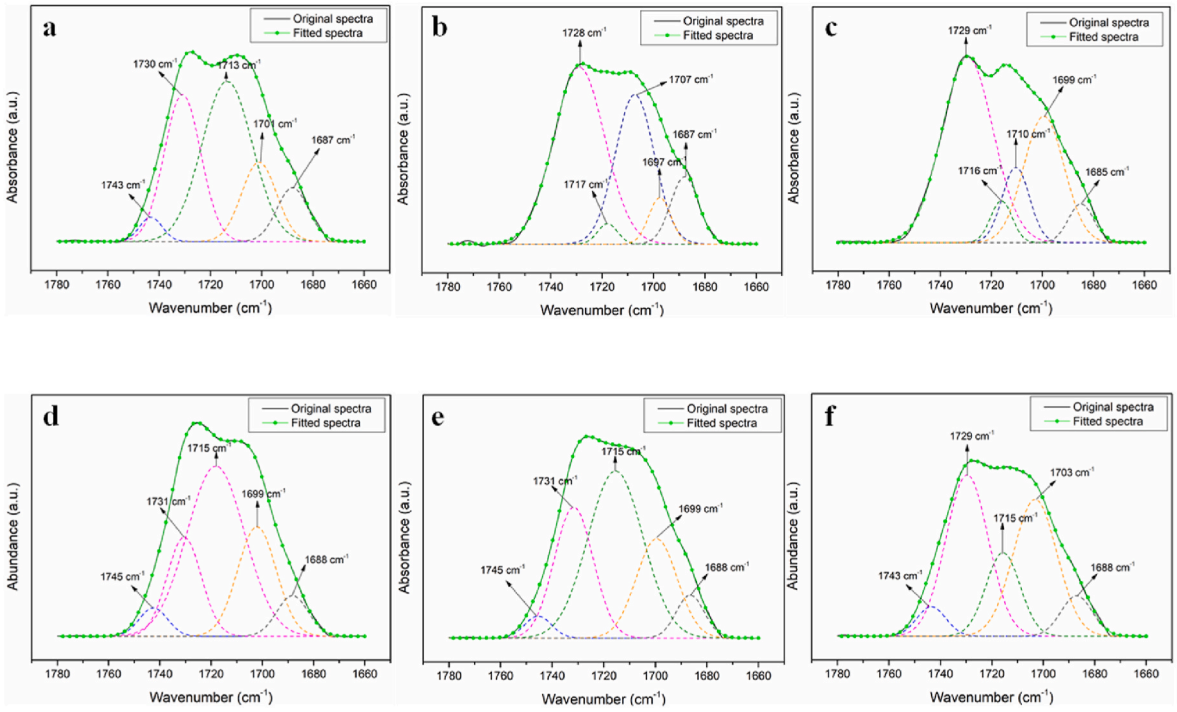

Fig. 4. ATR-FTIR spectra in the absorbance region of the carbonyl groups of the different LPAs. a, b and c are the 2.0, 2.5 and 3.0 LPA_{EPE} formulations and d, e and f are the LPA_{PPE} equivalents.

Table 6
Percentages of C=O urethane species in cured LPAs.

	NCO/OH	HS_t (%)	A	B	C	D	E	F	D + E + F
LPA_{EPE}	2.0:1	33.60	3.01	29.02	43.76	–	15.02	9.19	24.41
	2.5:1	38.74	2.24	29.56	39.15	8.10	10.46	10.49	29.04
	3.0:1	43.15	2.59	46.59	20.16	–	25.70	4.64	30.34
LPA_{PPE}	2.0:1	34.33	4.10	17.43	50.29	–	21.67	6.51	28.18
	2.5:1	39.52	2.92	25.23	45.67	–	20.19	5.98	26.17
	3.0:1	43.95	2.76	38.83	26.36	–	27.05	5.00	32.05

A: 1745-1743 cm^{-1} Free C=O in Soft Segment (%).
B: 1732-1729 cm^{-1}: Carbonyl-carbonyl interactions in Soft Segment (%).
C: 1714-1713 cm^{-1}: Free urethane C=O in Hard Segment (%).
D: 1706 cm^{-1}: H-bonded C=O in Soft-Hard Segment (%).
E: 1701-1697 cm^{-1}: H bonded urethane C=O in disordered Hard Segment (%).
F: 1686-1688 cm^{-1}: H bonded urethane C=O in ordered Hard Segment (%).

Table 7
Relevant parameters estimated for the determination of microphase of different formulations.

Sample	NCO:OH	z	X_{HB}	W_H	MP_W	SS_W	HS_W
LPA_{EPE}	2.0:1	0.336	0.316	0.257	0.086	0.750	0.250
	2.5:1	0.387	0.428	0266	0.103	0.716	0.284
	3.0:1	0.431	0.556	0.252	0.109	0.677	0.323
LPA_{PPE}	2.0:1	0.343	0.318	0.263	0.090	0.747	0.253
	2.5:1	0.395	0.323	0.307	0.121	0.726	0.274
	3.0:1	0.440	0.503	0.280	0.123	0.684	0.316

z is the HS_t fraction.

$$SS_w = MP_W + (1 - z) \quad \text{Equation 8}$$

$$HS_w = 1 - SS_W \quad \text{Equation 9}$$

Where X_{HB} is the weight fraction of H-bonded urethane and urea groups, A_{Hb} is the absorbance of the H-bonded C=O urethane groups (1708-1704 cm^{-1}, 1697-1694 cm^{-1} and 1688-1686 cm^{-1}) and urea groups (1675-1654 cm^{-1} and 1644-1630 cm^{-1}), A_{Fc} is the absorbance of free urethane C=O groups (1730-1728 cm^{-1}), the constant value K', with a value of 1.2 [34], is the extinction coefficient between H-bonded and free urethane C=O, and z is the theoretical Hard Segment (HS_t).

Based on the data in Table 7, the mass fraction of the H-bonded urethane groups (X_{HB}) increased with higher HS content. Additionally, the X_{HB} content was low across all formulations. This could be attributed to the cross-linked and sterically hindered structure of the lignin-based bio-polyol. Such a chemical configuration could inhibit hydrogen bonding between the carbonyl group of the urethane in the rigid segment chain and the NH urethane groups of adjacent rigid segment chains [35].

When analysing the mass fraction of the rigid segment mixed in the soft phase (W_H), a similar trend to that of X_{HB} was observed, where the W_H tended to increase with increasing the isocyanate content. Consequently, the mass fraction of the mixed phase also increased. This aligns with expectations, as increasing MDI content typically reduces the degree of phase separation, meaning more hard segments mix into the soft phase [34]. However, in the 3.0 formulations of both LPAs, a decreasing behaviour was observed obtaining the lowest value for LPA_{EPE}, while for LPA_{PPE}, the formulation 3.0 showed an intermediate value between the 2.0 and 2.5 formulations. Overall, the W_H and MP_W values of LPA_{EPE} were slightly lower than those for LPA_{PPE}, indicating that the former exhibited higher phase separation or lower miscibility between the HS and the SS. An explanation for this may lie in the nature of the lignin used to synthesise the PUs. Lignin from *Eucalyptus globulus*, which contains a higher number of syringyl groups in its structure, likely introduces greater steric hindrance, increasing phase separation and decreasing miscibility. Although this increased phase separation in LPA_{EPE} is relatively small, it could lead to improved mechanical properties in the PU [36].

The SS content predictably decreases with increasing HS content, which significantly impacts the final mechanical properties of the PU, as the SS provides flexibility and mobility to the polymer chains [37]. Therefore, it is necessary to find a balance between the chain mobility offered by the SS and the stiffness imparted by HS. Additionally, it should be noted that the theoretical HS content was higher than the calculated value, suggesting that the presence of lignin as well as its origin affected HS formation.

The ABES testing was carried out to measure the bonding strength of the different LPAs formulation. Such tests determine the tensile strength required to break the adhesive bond and provides an indication of the adhesive's shear strength [10]. Fig. 5a and b shows the shear strength test results for LPAs synthesised with EPE and PPE bio-polyols, employing different NCO:OH ratios.

A significant difference is evident between LPAs synthesised with EPE (Fig. 5a) and those synthesised with PPE (Fig. 5b). At NCO:OH ratios of 2.0 and 2.5, the LPAs synthesised with the PPE bio-polyol exhibited lower shear strength values. In contrast, when using a ratio of 3.0:1 the shear strength of the LPA increased rapidly, reaching 4.08 MPa at pressing time of 120 s.

The shear strength continued to increase, reaching 5.66 MPa at 180 s, except for the 2.0 and 2.5 LPA_{PPE} formulations. After this pressing time, the Beech veneer strips fractured, resulting in substrate failure. As seen in Fig. 5a, corresponding to LPA_{EPE} formulations. very similar high shear strength values were obtained regardless of the formulations used. This behaviour was probably caused by the unreacted isocyanate in these formulations, which interacted with the hydroxyl groups of the veneer strips, forming additional covalent bonds that distorted the results. This substrate failure also occurred in the LPA_{PPE} 3.0 formulation; however, in this case, the failure occurred at longer times. Considering the values presented in Table 7, there was no significant difference in HS_W and SS_W between the LPA_{EPE} and LPA_{PPE} formulations. Therefore, the previously mentioned unreacted isocyanate is the most plausible explanation for the unexpectedly high results obtained in the 2.0 and 2.5 LPA_{EPE} formulations.

Although pressing time is also influenced by temperature, to determine an optimal formulation, shear strength was evaluated using a pressing time of 120 s which is a common pressing time, for example, in particleboard industry [38], since times above 120 s are not profitable. At this pressing time, the highest shear strength value (3.58 MPa) was obtained with the 2.5:1 NCO:OH ratio in LPAs formulated with EPE, while a value of 4.08 MPa was achieved in PUs formulated with PPE using the 3.0:1 NCO:OH ratio. Although the shear strength of the 2.5:1 formulation of PPE was found to be significantly lower compared to that obtained from the same EPE formulation, as it was a value above 2 MPa [39], this ratio was chosen for formulating the LPAs based on the bio-polyols synthesised using CG (EPE_{CG} and PPE_{CG}).

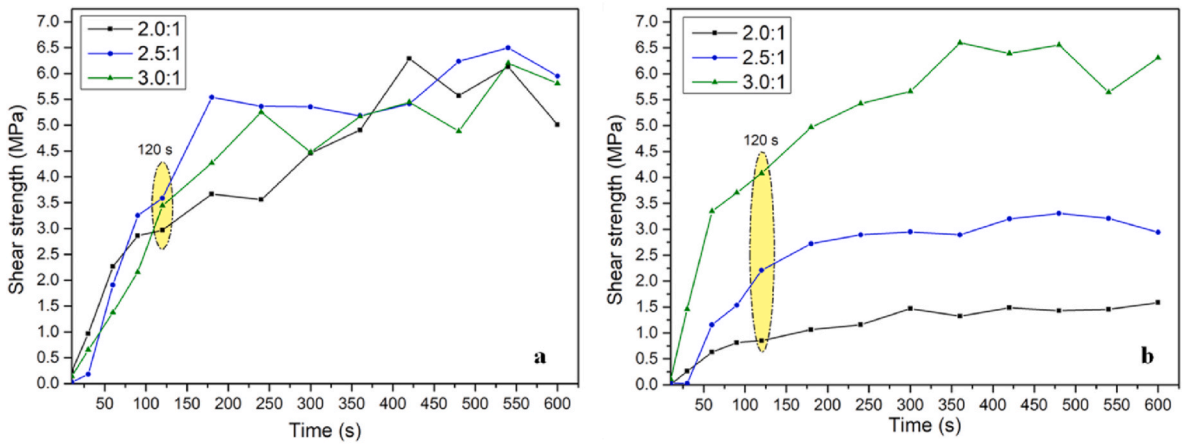

Fig. 5. Shear strength of lignin-based polyurethane adhesives; (a) LPA_{EPE}, (b) LPA_{PPE}.

3.3. Characterisation of LPA employing bio-polyols formulated with CG

Employing the respective quantities of reagents summarised in Table 3, two new LPAs were synthesised using the bio-polyols formulated with CG and NCO:OH ratio of 2.5:1, referred to as $LPA_{EPECG\_2.5}$ and $LPA_{PPECG\_2.5}$. A comparison was then made with the LPAs synthesised at the same NCO:OH ratio from the previous section.

The ATR-FTIR spectra of both cured LPAs, as well as the analysis of the region belonging to the carbonyl groups, are represented in Fig. S1 (Supplementary data), and Fig. 6a and b and respectively. The spectra exhibited the same characteristic bands as those described above. Notably, in this case as well, unreacted isocyanate was observed when the LPA was formulated using the bio-polyol from *Eucalyptus globulus* lignin. This, it can be confirming that due to the higher steric hindrance of the bio-polyol, part of the isocyanate was unable to react with the hydroxyl groups.

From the deconvolution of the carbonyl group region represented in Fig. 6a and b, the parameter X_{HB}, W_H, MP_W, SS_W and HS_W were calculated. The results obtained were summarised and compared with those for $LPA_{EPE\_2.5}$ and $LPA_{PPE\_2.5}$ and summarised in Table 8.

Compared to their respective counterparts, both LPAs synthesised using the bio-polyol formulated with CG showed a lower theoretical HS content and X_{HB}. Similarly, MP_W was lower, indicating that in this PUs, the amount of HS mixed into the soft phase was reduced, resulting in a greater micro-phase segregation. Such behaviour could be explained by the higher molecular weight of the EPE_{CG} and PPE_{CG} bio-polyols compared to EPE and PPE, which would promote the phase separation [40].

The structural analysis of polyurethanes was also performed using DSC. Fig. 7 presents the DSC thermograms of the polyurethane adhesives

Table 8
Relevant parameters estimated for the determination of microphase separation in GC-formulated LPAs.

	NCO:OH	z	X_{HB}	W_H	MP_W	SP_W	HS_W
$LPA_{EPE\_2.5}$	2.5:1	0.387	0.428	0.266	0.103	0.716	0.284
$LPA_{EPECG\_2.5}$	2.5:1	0.362	0.335	0.274	0.099	0.737	0.263
$LPA_{PPE\_2.5}$	2.5:1	0.395	0.323	0.307	0.121	0.726	0.274
$LPA_{PPECG\_2.5}$	2.5:1	0.346	0.303	0.269	0.093	0.747	0.253

$LPA_{EPE\_2.5}$, $LPA_{EPECG\_2.5}$, $LPA_{PPE\_2.5}$ and $LPA_{PPECG\_2.5}$.

The glass transition temperature (T_g) of a polyurethane is influenced by various factors related to the polyol, such as the I_{OH}, M_w, functionality, and the equivalent weight, which represent the ratio of molecular weight to functionality [41]. It is also well stablished that rigid structures, which restrict chain mobility, tend to increase the T_g of the polymer [25]. As expected for the synthesised lignin-based polyurethanes, the T_g of all systems was high due to the rigidity that lignin imparts to the system [10]. Furthermore, the T_g of a polyurethane is closely related to its structure; thus a linear polyurethane generally exhibits a higher T_g than branched ones, meaning that as the degree of crosslinking increases, the T_g of the polymer tends to decrease [42]. Another key factor is the phase mixing between the HS and SS of the polyurethane; greater phase separation tends to result in a higher T_g [43].

In relation to this study, given the similarity of the lignin and PEG/Gly ratios, and with identical NCO:OH ratios leading to a comparable degree of phase miscibility (Table (8), the resulting T_gs were notably similar. However, as shown in Fig. 7, the observed T_gs for each system

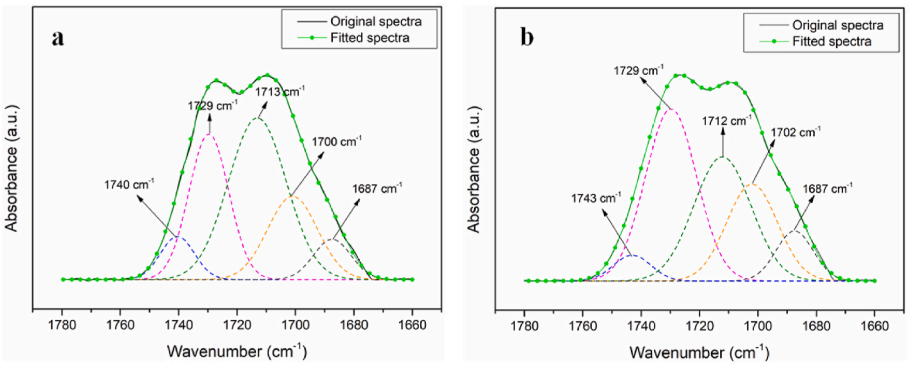

Fig. 6. ATR-FTIR spectra of the absorbance region of the carbonyl groups of $LPA_{EPECG\_2.5}$ (a) and $LPA_{PPECG\_2.5}$ (b) obtained through a Gaussian curve shape. The obtained R^2 values were above 0.999.

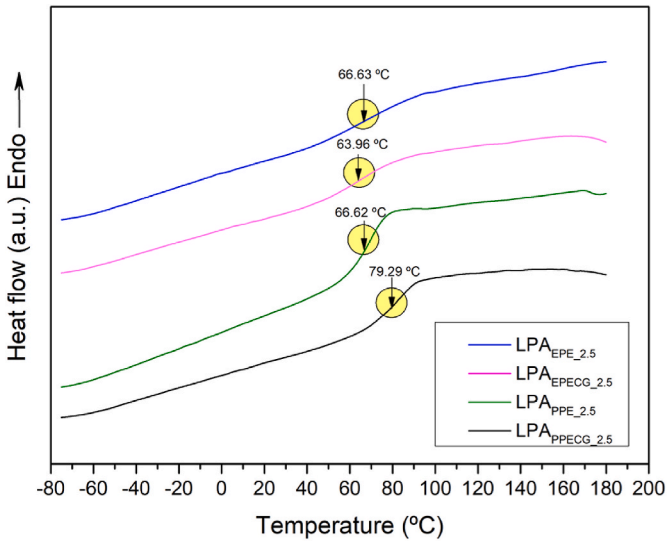

Fig. 7. DSC thermograms of the lignin based polyurethane adhesives.

varied, attributable to their distinct characteristics. For the LPAs synthesised with *Eucalyptus globulus* lignin, the T_g of $LPA_{EPE\_2.5}$ was slightly higher than that of $LPA_{EPECG\_2.5}$, despite the EPE bio-polyol having a lower EW than the EPE_{CG} bio-polyol, indicating a higher degree of crosslinking and lower microphase separation. Conversely, for the LPAs synthesised with *Pinus radiata* lignin, the higher T_g observed for $LPA_{PPECG\_2.5}$ can be attributed to increased microphase separation, resultinf from the higher molecular weight of the polyol used in the synthesis and a lower crosslinking of the system due to its higher EW value.

In Fig. 8, the shear strength of the $LPA_{EPECG\_2.5}$ and $LPA_{PPECG\_2.5}$ was measured and compared with their counterparts, $LPA_{EPE\_2.5}$ and $LPA_{PPE\_2.5}$. As expected, the results aligned with the conclusions obtained after studying the degree of microphase separation of LPAs, as the mechanical properties of polyurethanes can be improved by increasing the microphase separation [32]. Consequently, $LPA_{PPECG\_2.5}$ exhibited the highest shear strength of 6.06 MPa at 120 s, due to its lower weight fraction of the mixed phase and longer chains (EW), which reduce the concentration of urethane bonds and their cohesion. Together with its low functionality and high molecular weight, these factors contribute to an increase in the elasticity of the polyurethane [25], enabling the adhesive to withstand greater elongation before rupture. Nevertheless,

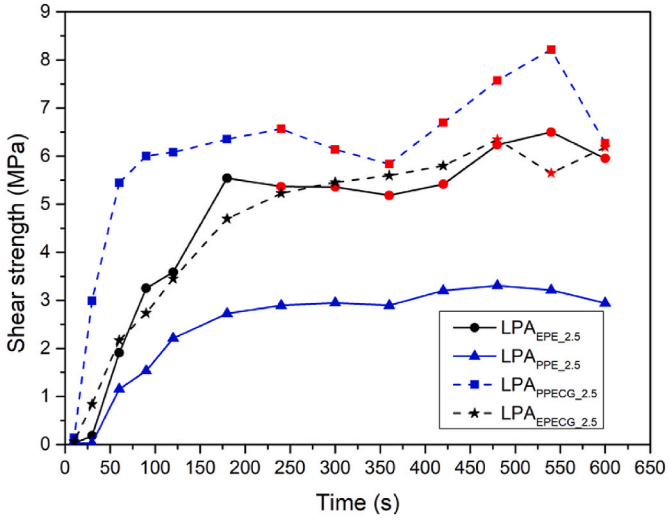

Fig. 8. Shear strength of lignin-based polyurethane adhesives. The red point indicated the substrate failure.

similar to $LPA_{EPE\_2.5}$, substrate failure occurred at pressing times higher than 180 s. On the other hand, it can be observed that the $LPA_{EPE\_2.5}$ and $LPA_{EPECG\_2.5}$ exhibited very similar shear strength values of 3.58 MPa and 3.44 MPa, respectively, despite the differences in microstructure and the molecular weight of the bio-polyols employed. Regarding the differences observed among the adhesives $LPA_{PPE\_2.5}$ and $LPA_{PPECG\_2.5}$ can be explained solely by the variations in molecular weights of the polyols, as well as the resulting differences in the microstructure of the polyurethanes.

The shear strength values obtained in this study were in the range of those reported by other authors. For instance Ref. [29], achieved a shear strength of 6.8 MPa using Kraft lignin and MDI with a NCO:OH ratio of 1.2:1. Additionally [10], used lignosulphonates along with MDI and different quantities of PEG200 to synthesise different wood adhesives, concludeding that the optimal formulation had an NCO:OH ratio of 2.1:1, yielding a shear strength value close to 3 MPa. Furthermore [44], studied the effect of lignin hydroxypropylation by synthesising various PU wood adhesives using kraft lignin (KL) and hydroxypropylated KL with MDI at a NCO:OH ratio of 1.1:1. Their findings indicated that the highest shear strength value was obtained with unmodified lignin (4.59 MPa), while hydroxpropylation improved elasticity and tensile strength but compromised shear strength. Meanwhile [45], obtained a wood PU adhesive based on oxyalkylated Kraft lignin, attaining a shear strength of 3.1 MPa with a NCO:OH ratio of 1.3:1.

The thermostability of the LPAs was studied through thermogravimetric analysis. According to the DTG curves represented in Fig. 9, the most significant weight loss for the samples occurred between 225 °C and 450 °C. Regardless of the polyol used in the LPA formulation, the degradation zones were the same although the maximum degradation temperatures varied slightly.

The first degradation zone, occurring between 225 °C and 310 °C, is associated with the H-bonded urethane groups of the HS [46], as well as the cleavage of unstable ether linkages of lignin (β-O-4, α-O-4 and 4-O-5) [47]. The second region, which exhibits the highest mass loss and occurs between 310 °C and 375 °C, is associated with the degradation of the soft segment of the polyurethane [28]. The final mass loss area, designated as region 3 (375 °C to 420 °C), is considered the degradation area of the diisocyanate and the aromatic rings of lignin [48]. A similar final residue was observed across all LPAs, due to the presence of lignin in the samples. Notably, the maximum degradation temperature during the initial mass loss phase was higher for $LPA_{EPE\_2.5}$ and $LPA_{EPECG\_2.5}$ compared to $LPA_{PPE\_2.5}$ and $LPA_{PPECG\_2.5}$, indicating greater stability of the formers. Generally, since the first degradation zone corresponds to the degradation of the H-bonded urethane groups, PUs with less amount of these, tend to be less stable, as less energy will be required to break them. Although this pattern was observed in the analysed samples, that is, the PUs synthesised with EPE showed a higher H-bond urethane

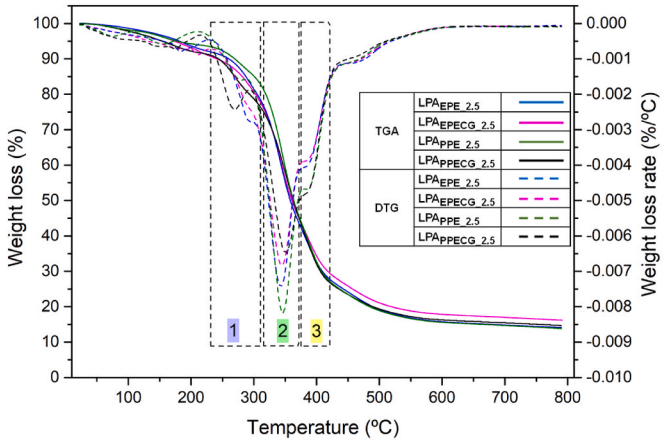

Fig. 9. TGA and DTG curves of the different LPAs.

groups, the slight difference compared to LPA_{PPE} PUs alone it cannot explain the greater stability of the former. This differences could be amplified by the degradation of ether linkages, which also occurs in the first degradation zone in polyurethanes containing lignin, which are more abundant in hardwoods such as *Eucalyptus globulus* than in softwood as *Pinus radiata* [49].

Using different heating rates (1, 2, 5 and 10 °C/min) and previously described isoconversional methods of OFW and KAS, the activation energy (E_a) for each system was calculated. In addition, the average lifetime of the LPAs was estimated through the OFW method, for which the pre-exponential factor A was determined. The calculation of both E_a and A was performed from the slope and the intercept of the plots of $\ln(\beta)$ and $\ln\left(\frac{\beta}{T_p^2}\right)$ versus 1000/Tp. In these graphs, the conversion rates from 5 % to 90 % were ploted for each system (Fig. S2). In all cases, as expected, as the heating rate increases, the degradation curve shifted towards higher temperatures. The final residue of each LPA was between 16.5 and 17 % ($LPA_{EPE\_2.5}$), 14–16 % ($LPA_{EPECG\_2.5}$), 13.9–15.8 % ($LPA_{PPE\_2.5}$) and 11.8–13.8 % ($LPA_{PPECG\_2.5}$).

From Table 9 and Fig. S3 and Table S1 from the supplementary data, it could be concluded that the model was well selected since linear and parallel straight lines and very high correlation coefficients were obtained. Nevertheless, in the case of the $LPA_{PPECG\_2.5}$ samples (Figs. S3d and S3h), the line corresponding to the 0.9 conversion was not properly fitted, and therefore, it was not considered for the calculation of the E_a and A.

According to the results outlined in Tables 9 and S1, and considering that the E_a represents the impediment to the degradation process [50], the degradation rate of synthesised LPAs will follow this order from the slowest to fastest for α = 0.05: $LPA_{EPE\_2.5} > LPA_{EPECG\_2.5} > LPA_{PPE\_2.5} > LPA_{PPECG\_2.5}$. Due to the nature of the bio-polyols, different behaviour was observed in the decomposition reaction mechanism between LPAs formulated with different bio-polyols, as shown in Fig. 10. The E_a followed a similar trend for both $LPA_{EPE\_2.5}$ and $LPA_{EPECG\_2.5}$, starting with a high value, decreasing to a minimum, and then increased again. In contrast, $LPAPPE_{2.5}$ and $LPA_{PPECG\_2.5}$ exhibited a different pattern, with the minimum E_a value appearing at the beginning, followed by an increase. However, in the case of $LPA_{PPECG\_2.5}$, the last two values tend to decrease because of the poor fitting.

Consequently, the values of the pre-exponential factor (A) estimated with the OFW method and presented in Table 10, followed the same tendency. This factor reflects the collision frequency between molecules, providing an indication of the availability of chemical groups which are susceptible to degradation [50]. Hence, a higher A value suggest that the polymer is more resistant to degradation. Therefore, $LPA_{EPE\_2.5}$ and $LPA_{EPECG\_2.5}$ polyurethanes exhibited greater stability at 5 % of conversion, while $LPA_{PPE\_2.5}$ and $LPA_{PPECG\_2.5}$ were more prone to degrade at this conversion rate.

Finally, the lifetime of the synthesised LPAs was evaluated, and the results are plotted in Fig. 11. Determining the lifetime of a material is crucial when developing a product with specific performance requirements for its intended application [51]. The estimation of the lifetime of the polymers can be determined employing the activation energies and the pre-exponential factors obtained through the OFW method. Usually, the lifetime estimation is conducted based on 5 % of weight loss or 5 % conversion [52]. However, the obtained data should be interpreted cautiously, as they reflect degradation in an inert atmosphere, and the lifetime will likely differ when the material is exposed to an oxidising atmosphere, where materials will degrade differently.

As expected, the obtained results aligned with the E_a values of the LPAs. Consequently, the LPA with the highest lifetime expectation was $LPA_{EPE\_2.5}$, followed by $LPA_{EPECG\_2.5}$, then $LPA_{PPE\_2.5}$ and finally

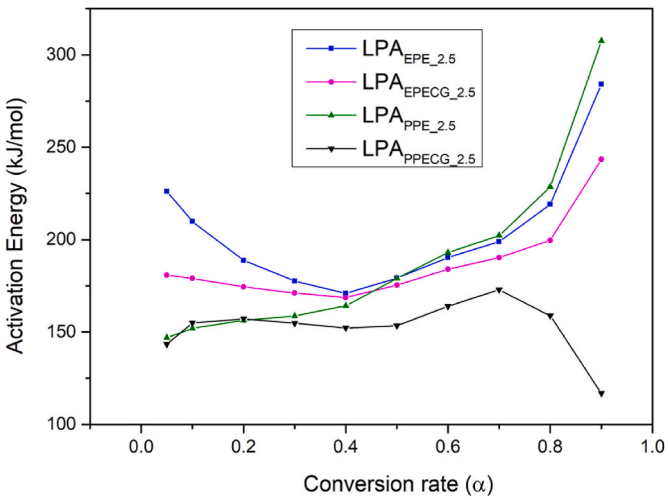

Fig. 10. E_a calculated through OFW method vs. α

Table 10
Preexponential factor (A) of the PU samples for the decomposition obtained through the OFW method.

α	A (min^{-1})			
	$LPA_{EPE\_2.5}$	$LPA_{EPECG\_2.5}$	$LPA_{PPE\_2.5}$	$LPA_{PPECG\_2.5}$
0.05	3.7E+18	9.7E+11	9.8E+08	6.6E+10
0.1	1.5E+17	2.1E+14	8.4E+11	2.3E+11
0.2	2.1E+15	1.0E+14	2.3E+12	5.0E+11
0.3	2.0E+14	5.2E+13	3.6E+12	3.5E+11
0.4	4.6E+13	2.8E+13	9.3E+12	2.1E+11
0.5	8.6E+13	6.9E+13	1.2E+14	2.0E+11
0.6	7.1E+14	2.1E+14	1.1E+15	9.7E+11
0.7	1.9E+15	3.5E+14	3.8E+15	3.1E+12
0.8	1.8E+16	5.4E+14	1.4E+17	1.1E+11
0.9	3.0E+17	6.9E+16	3.1E+21	2.3E+07

Table 9
Activation energies (E_a) (kJ/mol) and correlation coefficients of the linear regression of the PU samples for the decomposition obtained through the OFW method.

α	$LPA_{EPE\_2.5}$		$LPA_{EPECG\_2.5}$		$LPA_{PPE\_2.5}$		$LPA_{PPECG\_2.5}$	
	R^2	E_a	R^2	E_a	R^2	E_a	R^2	E_a
0.05	0.9976	226.0	0.9830	180.8	0.9432	146.9	0.9970	143.4
0.1	0.9989	209.8	0.9849	179.0	0.9464	152.0	0.9995	154.9
0.2	0.9995	188.8	0.9899	174.4	0.9526	156.3	0.9992	157.1
0.3	0.9998	177.6	0.9923	171.1	0.9508	158.7	0.9972	154.8
0.4	0.9999	171.0	0.9920	168.7	0.9481	164.2	0.9947	152.2
0.5	0.9999	179.2	0.9893	175.4	0.9467	179.1	0.9919	153.4
0.6	0.9997	190.3	0.9926	184.0	0.9689	193.0	0.9900	164.0
0.7	0.9991	198.9	0.9964	190.3	0.9785	202.2	0.9762	172.9
0.8	0.9913	219.1	0.9939	199.6	0.9468	228.5	0.8829	158.8
0.9	0.9677	284.1	0.9929	243.4	0.9412	307.5	0.4439[a]	116.9

[a] Not considered for calculating the average.

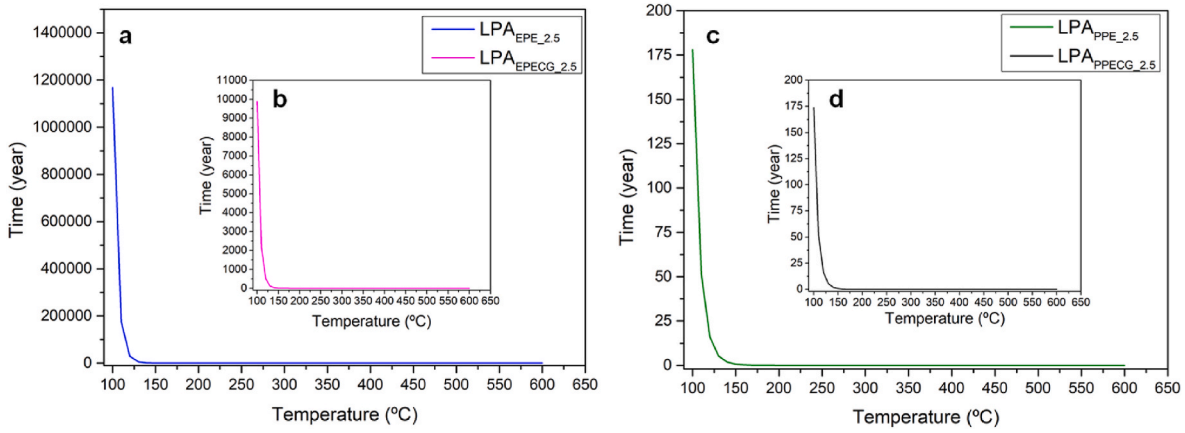

Fig. 11. Estimated lifetime of $LPA_{EPE\_2.5}$ (a), $LPA_{EPECG\_2.5}$ (b), $LPA_{PPE\_2.5}$ (c) and $LPA_{PPECG\_2.5}$ (d).

$LPA_{PPECG\_2.5}$. It is worth noting that the difference between $LPA_{EPE\_2.5}$ and $LPA_{EPECG\_2.5}$ was significant, due to the large disparity in their E_a values, whereas the difference between $LPA_{PPE\_2.5}$ and $LPA_{PPECG\_2.5}$ was minimal. Additionally, it was observed that as the temperature increased, the degradation of the polymers accelerated considerably in all cases.

4. Conclusions

This study demonstrated the potential of bio-polyols synthesised through the liquefaction process of lignin with polyhydric alcohols (PEG and Glycerol) using microwave irradiation for formulating PU adhesives. The results indicated that it is feasible to substitute commercial glycerol with non-purified crude glycerol obtained from used vegetable oil. It was determined that the origin of the lignin significantly affected the properties of the lignin-based polyurethane. On the one hand, when the bio-polyol derived from *Eucalyptus globulus* (hardwood) lignin was used, isocyanate remained unreacted in all cases, whereas with its counterpart derived from *Pinus radiata* (softwood) lignin did not exhibit this behaviour, likely due to the higher steric hindrance associated with the former. Furthermore, the choice of glycerol also had a substantial impact on the microstructure of the LPAs, as the bio-polyols synthesised using crude glycerol exhibited higher molecular weights, which favoured greater phase separation.

In terms of thermal stability, it was found that the lignin source played an important role, since despite the LPAs showed similar H-bonded urethane groups, the PUs synthesised with EPE bio-polyol displayed greater stability attributed to a higher concentration of aryl ether bonds within their structure. Consequently, the estimated lifetime of the LPAs at 5 % degradation followed the same order $LPA_{EPE\_2.5} > LPA_{EPECG\_2.5} > LPA_{PPE\_2.5} > LPA_{PPECG\_2.5}$.

Nevertheless, further investigation into how lignin influences the microstructure of these polyurethanes is warranted, as discrepancies have been observed between the expected and obtained results concerning phase miscibility in higher NCO:OH formulations (3.0:1). Additionally, it would be valuable to analyse the behaviour of lignin with lower polydispersity index and greater homogeneity in such systems.

CRediT authorship contribution statement

Fabio Hernández-Ramos: Writing – original draft, Validation, Methodology, Investigation, Formal analysis, Data curation, Conceptualization. **Bruno Esteves:** Visualization, Validation, Supervision, Data curation. **Luísa Carvalho:** Visualization, Validation, Supervision, Data curation. **Jalel Labidi:** Validation, Supervision, Methodology, Funding acquisition, Data curation. **Xabier Erdocia:** Validation, Supervision, Methodology, Formal analysis, Data curation, Conceptualization.

Declaration of competing interest

The authors declare that they have no known competing financial interests or personal relationships that could have appeared to influence the work reported in this paper.

Acknowledgements

The authors wish to acknowledge the financial support provided by the Basque Government (IT1498-22) and the national funds FCT/MCTES (PIDDAC): LEPABE, UIDB/00511/2020 (DOI: 10.54499/UIDB/00511/2020), ALiCE, LA/P/0045/2020 (DOI: 10.54499/LA/P/0045/2020) and CERNAS (UIDB/00681/2020 DOI: 10.54499/UIDB/00681/2020). They also express their gratitude to SGIker for their outstanding technical support and kindness. Fabio Hernández-Ramos would like to extend his utmost gratitude to the Polytechnic Institute of Viseu for enabling his doctoral stay, resulting in the completion of this article, and especially to Professor Bruno Miguel de Morais for his exceptional hospitality.

Appendix A. Supplementary data

Supplementary data to this article can be found online at https://doi.org/10.1016/j.ijadhadh.2024.103889.

Data availability

No data was used for the research described in the article.

References

[1] Haridevan H, Evans DAC, Ragauskas AJ, Martin DJ, Annamalai PK. Valorisation of technical lignin in rigid polyurethane foam: a critical evaluation on trends, guidelines and future perspectives. Green Chem 2021. https://doi.org/10.1039/d1gc02744a.

[2] Ponnusamy VK, Nguyen DD, Dharmaraja J, Shobana S, Banu JR, Saratale RG, et al. A review on lignin structure, pretreatments, fermentation reactions and biorefinery potential. Bioresour Technol 2019. https://doi.org/10.1016/j.biortech.2018.09.070.

[3] Quinsaat JEQ, Feghali E, Van De Pas DJ, Vendamme R, Torr KM. Preparation of mechanically robust bio-based polyurethane foams using depolymerized native lignin. ACS Appl Polym Mater 2021. https://doi.org/10.1021/acsapm.1c01081.

[4] Mahmood N, Yuan Z, Schmidt J, Xu C. Depolymerization of lignins and their applications for the preparation of polyols and rigid polyurethane foams: a review. Renew Sustain Energy Rev 2016;60:317–29. https://doi.org/10.1016/j.rser.2016.01.037.

[5] Stachak P, Łukaszewska I, Hebda E, Pielichowski K. Recent advances in fabrication of non-isocyanate polyurethane-based composite materials. Materials 2021;14. https://doi.org/10.3390/ma14133497.

[6] Li YY, Luo X, Hu S. Lignocellulosic biomass-based polyols for polyurethane applications. Bio-based Polyols and Polyurethanes 2015:1–79. https://doi.org/10.1007/978-3-319-21539-6.

[7] Perez-arce J, Centeno-pedrazo A, Labidi J, Ochoa-gomez JR, Garcia-suarez EJ. Lignin-based polyols with controlled microstructure by cationic ring opening polymerization. Polymers 2021;13:1–12. https://doi.org/10.3390/polym13040651.

[8] Zhao W, Liang Z, Feng Z, Xue B, Xiong C, Duan C, et al. New kind of lignin/polyhydroxyurethane composite: green synthesis, smart properties, promising applications, and good reprocessability and recyclability. ACS Appl Mater Interfaces 2021;13:28938–48. https://doi.org/10.1021/acsami.1c06822.

[9] Alinejad M, Henry C, Nikafshar S, Gondaliya A, Bagheri S, Chen N, et al. Lignin-based polyurethanes: opportunities for bio-based foams, elastomers, coatings and adhesives. Polymers 2019. https://doi.org/10.3390/polym11071202.

[10] Magina S, Gama N, Carvalho L, Barros-Timmons A, Evtuguin DV. Lignosulfonate-based polyurethane adhesives. Materials 2021;14:1–18. https://doi.org/10.3390/ma14227072.

[11] Upton BM, Kasko AM. Strategies for the conversion of lignin to high-value polymeric materials: review and perspective. Chem Rev 2016;116:2275–306. https://doi.org/10.1021/acs.chemrev.5b00345.

[12] Laurichesse S, Avérous L. Chemical modification of lignins: towards biobased polymers. Prog Polym Sci 2014;39:1266–90. https://doi.org/10.1016/j.progpolymsci.2013.11.004.

[13] Gonçalves S, Ferra J, Paiva N, Martins J, Carvalho LH, Magalhães FD. Lignosulphonates as an alternative to non-renewable binders in wood-based materials. Polymers 2021;13:1–29. https://doi.org/10.3390/polym13234196.

[14] Gosz K, Kosmela P, Hejna A, Gajowiec G, Piszczyk Ł. Biopolyols obtained via microwave-assisted liquefaction of lignin: structure, rheological, physical and thermal properties. Wood Sci Technol 2018;52:599–617. https://doi.org/10.1007/s00226-018-0991-4.

[15] Donadini R, Boaretti C, Lorenzetti A, Roso M, Penzo D, Dal Lago E, et al. Chemical recycling of polyurethane waste via a microwave-assisted glycolysis process. ACS Omega 2023;8:4655–66. https://doi.org/10.1021/acsomega.2c06297.

[16] Heiran R, Ghaderian A, Reghunadhan A, Sedaghati F, Thomas S, Haghighi AH. Glycolysis: an efficient route for recycling of end of life polyurethane foams. J Polym Res 2021;28. https://doi.org/10.1007/s10965-020-02383-z.

[17] Hernández-Ramos F, Novi V, Alriols MG, Labidi J, Erdocia X. Optimisation of lignin liquefaction with polyethylene glycol/glycerol through response surface methodology modelling. Ind Crops Prod 2023;198. https://doi.org/10.1016/j.indcrop.2023.116729.

[18] Hernández-Ramos F, Alriols MG, Antxustegi MM, Labidi J, Erdocia X. Valorisation of crude glycerol in the production of liquefied lignin bio-polyols for polyurethane formulations. Int J Biol Macromol 2023;247. https://doi.org/10.1016/j.ijbiomac.2023.125855.

[19] Costa NA, Pereira J, Ferra J, Cruz P, Martins J, Magalhães FD, et al. Evaluation of bonding performance of amino polymers using ABES. J Adhes 2014;90:80–8. https://doi.org/10.1080/00218464.2013.784693.

[20] Ozawa T. A new method of analyzing thermogravimetric data. Bull Chem Soc Jpn 1965;38:1881–6. https://doi.org/10.1246/bcsj.38.1881.

[21] Vyazovkin S. Kissinger method in kinetics of materials: things to beware and Be aware of. Molecules 2020;25. https://doi.org/10.3390/molecules25122813.

[22] Ionescu M. Polyols. In: De Gruyter, editor. Polyols for polyrethanes; 2019. p. 1–10. https://doi.org/10.1515/9783110644104-001. Boston, Berlin.

[23] Hu S, Luo X, Li Y. Polyols and polyurethanes from the liquefaction of lignocellulosic biomass. ChemSusChem 2014;7:66–72. https://doi.org/10.1002/cssc.201300760.

[24] Li YY, Luo X, Hu S. Introduction to bio-based polyols and polyurethanes. Bio-based Polyols and Polyurethanes; 2015. p. 1–79. https://doi.org/10.1007/978-3-319-21539-6.

[25] Ionescu M. Relationships between the oligo-polyol structure and polyurethane properties. Polyols for polyurethanes. Boston, Berlin: De Gruyter; 2019. p. 307–20. https://doi.org/10.1515/9783110644128-011.

[26] Ren F, Zhou R, Sun F, Ma H, Zhou Z, Xu W. Blocked isocyanate silane modified Al2O3/polyamide 6 thermally conductive and electrical insulation composites with outstanding mechanical properties. RSC Adv 2017;7:29779–85. https://doi.org/10.1039/c7ra04454b.

[27] Fuensanta M, Martín-Martínez JM. Viscoelastic and adhesion properties of new poly(ether-urethane) pressure-sensitive adhesives. Front Mech Eng 2020;6:1–10. https://doi.org/10.3389/fmech.2020.00034.

[28] Cinelli P, Anguillesi I, Lazzeri A. Green synthesis of flexible polyurethane foams from liquefied lignin. Eur Polym J 2013;49:1174–84. https://doi.org/10.1016/j.eurpolymj.2013.04.005.

[29] Nacas AM, Ito NM, Sousa RRD, Spinacé MA, Dos Santos DJ. Effects of NCO:OH ratio on the mechanical properties and chemical structure of Kraft lignin–based polyurethane adhesive. J Adhes 2017;93:18–29. https://doi.org/10.1080/00218464.2016.1177793.

[30] Fuensanta M, Martín-Martínez JM. Structural and viscoelastic properties of thermoplastic polyurethanes containing mixed soft segments with potential application as pressure sensitive adhesives. Polymers 2021;13. https://doi.org/10.3390/polym13183097.

[31] Liu Y, Liu L, Liang Y. Relationship between structure and dynamic mechanical properties of thermoplastic polyurethane elastomer containing bi-soft segment. J Appl Polym Sci 2020;137:1–9. https://doi.org/10.1002/app.49414.

[32] Gholami M, Haddadi-Asl V, Jouibari IS. A review on microphase separation measurement techniques for polyurethanes. J Plast Film Sheeting 2022;38:502–41. https://doi.org/10.1177/87560879221088939.

[33] Fuensanta M, Martín-Martínez JM. Influence of the hard segments content on the structure, viscoelastic and adhesion properties of thermoplastic polyurethane pressure sensitive adhesives. J Adhes Sci Technol 2020;34:2652–71. https://doi.org/10.1080/01694243.2020.1780774.

[34] Niemczyk A, Piegat A, Sonseca Olalla Á, El Fray M. New approach to evaluate microphase separation in segmented polyurethanes containing carbonate macrodiol. Eur Polym J 2017;93:182–91. https://doi.org/10.1016/j.eurpolymj.2017.05.046.

[35] Luo X, Mohanty A, Misra M. Lignin as a reactive reinforcing filler for water-blown rigid biofoam composites from soy oil-based polyurethane. Ind Crops Prod 2013;47:13–9. https://doi.org/10.1016/j.indcrop.2013.01.040.

[36] Kojio K, Nozaki S, Takahara A, Yamasaki S. Influence of chemical structure of hard segments on physical properties of polyurethane elastomers: a review. J Polym Res 2020;27:64–7. https://doi.org/10.1007/s10965-020-02090-9.

[37] Arévalo-Alquichire S, Morales-Gonzalez M, Navas-Gómez K, Diaz LE, Gómez-Tejedor JA, Serrano MA, et al. Influence of polyol/crosslinker blend composition on phase separation and thermo-mechanical properties of polyurethane thin films. Polymers 2020;12. https://doi.org/10.3390/polym12030666.

[38] Gonçalves C, Pereira J, Paiva N, Ferra J, Martins J, Magalhaes F, et al. Impact of the synthesis procedure on urea-formaldehyde resins prepared by alkaline-acid process. Ind Eng Chem Res 2019;58:5665–76. https://doi.org/10.1021/acs.iecr.8b06043.

[39] Frihart CR, Lorenz L. Standard test method ASTM D 7998-19 for the cohesive strength development of wood adhesives. J Vis Exp 2020;2020:1–6. https://doi.org/10.3791/61184.

[40] Lee D-K, Tsai H-B, Tsai R-S, Chen PH. Preparation and properties of transparent thermoplastic segmented polyurethanes derived from different polyols. Polym Eng Sci 2007;47:695–701. https://doi.org/10.1002/pen.20742.

[41] Ionescu M. 3. General characteristics of oligo-polyols 2019;1+2:27–46. https://doi.org/10.1515/9783110644104-003 [Set Polyols Polyurethanes.

[42] Kritskaya DA, Kurmaz SV, Kochneva IS. Glass transition temperature and architecture of branched poly(methyl methacrylates). Polym Sci 2007;49:1120–8. https://doi.org/10.1134/S0965545X07100094.

[43] Son TW, Won D, Lim Kyoo S. Thermal and phase behavior of polyurethane based on chain extender, 2,2-Bis-[4-(2-hydroxyethoxy)phenyl]propane. Polym J 1999;31:563–8.

[44] Gouveia JR, Antonino LD, Garcia GES, Tavares LB, Santos ANB, Santos DJ do. Kraft lignin-containing polyurethane adhesives: the role of hydroxypropylation on thermomechanical properties. J Adhes 2021;97:1423–39. https://doi.org/10.1080/00218464.2020.1784148.

[45] Vieira FR, Gama N, Magina S, Barros-Timmons A, Evtuguin DV, Pinto PCOR. Polyurethane adhesives based on oxyalkylated kraft lignin. Polymers 2022;14. https://doi.org/10.3390/polym14235305.

[46] D'Souza J, Camargo R, Yan N. Polyurethane foams made from liquefied bark-based polyols. J Appl Polym Sci 2014;131:1–10. https://doi.org/10.1002/app.40599.

[47] Zhang C, Wu H, Kessler MRK. High bio-content polyurethane composites with urethane modified lignin as filler. Polymer (Guildf) 2015;69:52–7. https://doi.org/10.1016/j.polymer.2015.05.046.

[48] Tavares LB, Boas CV, Schleder GR, Nacas AM, Rosa DS, Santos DJ. Bio-based polyurethane prepared from Kraft lignin and modified castor oil. Express Polym Lett 2016;10:927–40. https://doi.org/10.3144/EXPRESSPOLYMLETT.2016.86.

[49] Erdocia X, Hernández-ramos F, Morales A, Izaguirre N, Hoyos-martínez PL De, Labidi J. Lignin extraction and isolation methods. In: Lignin-based mater. Biomed. Appl. Elsevier Inc.; 2021. p. 61–104. https://doi.org/10.1016/c2019-0-01345-3.

[50] Batista NL, Costa ML, Iha K, Botelho EC. Thermal degradation and lifetime estimation of poly(ether imide)/carbon fiber composites. J Thermoplast Compos Mater 2015;28:265–74. https://doi.org/10.1177/0892705713484740.

[51] Flynn JH. A critique of lifetime prediction of polymers by thermal analysis. J Therm Anal Calorim 1995;44:499–512. https://doi.org/10.1007/BF02636139.

[52] Núñez L, Fraga F, Núñez MR, Villanueva M. Lifetime prediction of the epoxy system badge n = 0/1,2 DCH by thermogravimetric analysis. J Appl Polym Sci 2000;78:1239–44. https://doi.org/10.1002/1097-4628(20001107)78:6<1239::aid-app90>3.0.co;2-x.